Clays and Clay Minerals, Vol. 58, No. 5, 596–605, 2010.

SYNTHESIS AND CHARACTERIZATION OF Zn-Al LAYERED DOUBLE HYDROXIDES INTERCALATED WITH 1- TO 19-CARBON CARBOXYLIC ACID ANIONS

THOMAS KUEHN[1] AND HERBERT POELLMANN[2]

[1] Soil Science, Martin Luther University Halle-Wittenberg, Weidenplan 14, 06108 Halle, Germany
[2] Mineralogy/Geochemistry, Martin Luther University Halle-Wittenberg, Von-Seckendorff-Platz 3, 06120 Halle, Germany

Abstract—Layered double hydroxides (LDHs) are layered ion exchangers, with a large surface-charge density, which react easily with organic anions. Various types of organics are rapidly substituted in the interlayer space of inorganic precursor LDHs. ZnAl-LDHs were intercalated with 1- to 19-carbon monocarboxylic acid anions by anion exchange of NO_3^--saturated LDH precursor phases in order to study the dependence of exchange reactions on synthesis parameters (temperature, pH, and interlayer anion). The carboxylic acid anion-LDHs synthesized were characterized using X-ray diffraction, infrared spectroscopy, thermal analysis, scanning electron microscopy, chemical analysis, and N_2 adsorption. Carboxylic anion quantities in excess of the LDH anion exchange capacity easily replaced exchangeable nitrate anions at moderate pH. The intercalated LDH interlayer space depended on the alkyl chain length and orientation (inclination angle) of the carboxylic-acid anion. The lattice parameter c_0 ranged from 3.4 to 13.5 nm, but the a_0 lattice parameter remained constant at 0.31 nm. Crystallographic analyses indicated a monomolecular arrangement of intercalated short-chain fatty-acid anions. At pH < 7, intercalated long-chain carboxylates showed a preferred bimolecular interlayer orientation. Carboxylic-acid anion exchange with LDHs at pH 7 resulted in the formation of two different sets of basal spacings, which indicated the coexistence of LDHs intercalated with monomolecular and bimolecular arrangements of interlayer carboxylic compounds.

Thermal treatment of the carboxylic acid anion-intercalated LDHs indicated stability up to ~140ºC. The release of interlayer water led to distortion of the crystallographic units and resulted in smaller basal spacings without collapse of the layered structure. Heat treatment re-oriented alkyl-chain carbon carboxylates (with >10 carbons) to a more upright interlayer position.

Key Words—Anion Exchange, Carboxylic Acid Anion, Hydrotalcite, LDH.

INTRODUCTION

Layered double hydroxides (LDHs), also known as anionic clays, metal-metal hydroxy salts, or hydrotalcite-like compounds, are natural and synthetic compounds that consist of different chemical and structural alternating layers. Positively charged brucite-like main layers are balanced by exchangeable interlayer anions, and water molecules also occupy the interlayer space (Bish, 1980). In addition, large monovalent cations can be substituted into the interlayer (Cooper and Hawthorne, 1996). The charge on the main layer, $(Me(OH))^{n+}$, is derived from partial replacement of divalent cations (*e.g.* Mg^{2+}) by trivalent cations (*e.g.* Al^{3+}, Fe^{3+}, Cr^{3+}). The simplified chemical formula is $[Me(II)_{1-x}Me(III)_x(OH)_2]^{x+}[A_{x/r}\cdot nH_2O]^{x-}$, where *Me*(II) and *Me*(III) are the di- and trivalent cations in the octahedral sites of the main layer and $A_{x/r}$ is the exchanged anion. The limiting factors for incorporation of metal cations in the brucite-like layers are the ionic radii of Me^{2+} and Me^{3+}, which generally vary between 0.06 and 0.08 nm for the divalent cations and between 0.06 and 0.07 nm for the trivalent cations (Roy *et al.*, 2001). The most prominent exceptions are Al^{3+} and Ca^{2+} with ionic radii of 0.05 nm and 0.1 nm, respectively. According to Kloprogge *et al.* (2002), the most reliable limits for LDH-structure formation are based on the trivalent to divalent metal ratio x, which is in the range $0.17 \leqslant x \leqslant 0.33$. The synthesis, structure, and properties of LDHs, especially the permanent anion exchange capacity (AEC), have been studied extensively (*e.g.* Cavani *et al.*, 1991; Ogawa and Kaiho, 2002; Prasanna *et al.*, 2009). Many LDHs have been synthesized for different advanced-material applications because the chemical composition of both LDH main layers and interlayers can be varied. The LDHs are used as adsorbents, antacid drugs, catalysts, anion exchangers, and heavy metal- and pharmaceutical-reservoir minerals (Choudhary *et al.*, 2003; Hansen *et al.*, 2009; Khan and O'Hare, 2002; Poellmann, 2007; Yang *et al.*, 2005). Recent studies have focused on interlayer-space manipulation with large organic anions and pharmaceutical compound substitutions in LDHs (Reinholdt and

* E-mail address of corresponding author:
thomas.kuehn@landw.uni-halle.de
DOI: 10.1346/CCMN.2010.0580502

Kirkpatrick, 2006; Xu and Bratermann, 2007). Those properties are desirable for the use of LDHs as molecular sieves or synthetic pharmaceutical-reservoir minerals with specific, predefined properties (Zhao and Vance, 1998).

The present study focused on the synthesis of zinc-aluminum LDHs (ZnAl-LDHs) with carboxylic acid anions introduced into the interlayers by anion exchange. The size of the LDH interlayer space varies with the size and position of the intercalated molecule. Interlayer organic anions can be arranged in closely packed monolayers or bilayers (Itoh *et al.*, 2003). Intercalation of selected aromatic and aliphatic carboxylate anions into LDH structures has been reported widely, but LDH anion-exchange experiments using different chain-length, saturated aliphatic carboxylic acids have been little reported (Anbarasan *et al.*, 2005; Carlino, 1997; Wypych *et al.*, 2005). The purpose of this work was to evaluate the intercalation of carboxylic acids with 1- to 20-carbon alkyl chains into LDHs in order to produce nanoparticles with well defined properties (*e.g.* porosity and specific surface area). The effect of carboxylic acid alkyl-chain length and synthesis parameters (*e.g.* pH, concentration, temperature) on interlayer space development was, therefore, investigated. A ZnAl-LDH nitrate precursor phase was used to study carboxylate anion exchange reactions using X-ray diffraction (XRD), Fourier-transform infrared (FTIR) spectroscopy, and elemental analysis. Thermal decomposition and the different hydration stages of carboxylate-intercalated LDHs were investigated by thermogravimetry (TG) and thermal XRD using a heating chamber.

METHODS

Sample preparation

Zn-Al hydroxide precursor phases were synthesized by the co-precipitation method according to Reichle (1986). An aqueous solution of 0.5 M $Zn(NO_3)_2{\cdot}6H_2O$ and 0.3 M $Al(NO_3)_3{\cdot}9H_2O$ was prepared and the pH was adjusted to 7.3−7.5 by dropwise addition of an aqueous NaOH solution (1 M) under constant stirring. Greater pH values led to the formation of ZnO as a minor phase and lower pH resulted in less crystalline LDH-like phases. Nitrate was selected as the counterion because it can be more easily removed from the interlayer than chloride or sulfate anions. Although preliminary exchange experiments using chloride and sulfate as counterions permitted interlayer organic anion intercalation, very large excesses of organic acids were necessary to avoid mixed-LDH phases with precursor anion impurities. The solutions were aged in polyethylene bottles at 45ºC for 7 days, filtered, and washed three times with deionized water to eliminate excess salt. Carboxylate/LDH anion-exchange reactions were performed by adding sodium carboxylate solutions at different initial pH to 20 mL aqueous LDH- precursor suspensions. The mixtures were equilibrated in a shaker at 45ºC for 7 days. After filtration and washing, the resulting LDHs were dried over $CaCl_2{\cdot}6H_2O$ in a desiccator at 35% relative humidity (r.h.). All synthesis, washing, and drying procedures were performed under a nitrogen atmosphere in a glove box using boiled, deionized water to prevent carbonate anion incorporation. Interlayer carbonate anions in LDHs complicate later anion exchange reactions. The chemicals used were of reagent grade. Aluminum nitrate, butanoic-acid sodium salt, pentanoic-acid sodium salt, hexanoic acid, and heptanoic acid were supplied by Merck (Darmstadt, Germany). The propanoic-acid sodium salt was from Sigma Aldrich (Steinheim, Germany). All the other chemicals used were provided by Fluka (Buchs, Germany).

Characterization

X-ray crystallographic analyses were carried out using an X'Pert Pro MPD diffractometer (PANalytical, Almelo, Netherlands) with CuKα radiation and 99.99% silicon (a_0 = 0.54308 nm, 99.99%) as an internal standard. The samples were prepared as wet pastes, dried at 35% r.h., and scanned in step-scan mode using a step size of 0.02º2θ and a counting time of 10.2 s/step. Least-squares refinements of X-ray powder data were performed using a trigonal lattice (hexagonal axes) with $R\bar{3}m/R3m$ rhombohedral symmetry. The morphology of carboxylate-LDHs was analysed by scanning electron microscopy (SEM; JSM6300, JEOL, Tokyo, Japan). Thermal stability was examined on powder samples using a Seiko 320U TG/DTA thermogravimetric and differential thermal analyzer (Seiko Instruments Inc., Chiba, Japan) and an Anton Paar HTK-16 heating chamber (Anton Paar GmbH, Graz, Austria) with a typical heating rate of 5 K min^{-1} under an air/nitrogen atmosphere. Chemical analyses for Zn and Al were carried out using a Plasmaquant 110 ICP-OES (Analytic Jena, Jena, Germany) and C, H, and N analyses were performed using a Leco CHNS-932 elemental analyzer (Leco Corporation, St. Joseph, Michigan, USA). Due to polymerization of the long-chain carboxylate anions, the organic LDHs prepared using carboxylates with >13-carbon alkyl chains required 1 h of treatment at 250ºC before dissolution in 1 M nitric acid. The FTIR spectra (400−4000 cm^{-1}) were recorded from disks consisting of 1 mg of sample to 300 mg of KBr, using a Bruker Equinox 55 FTIR (Bruker Optics, Inc., Billerica, Massachusetts, USA) spectrometer. A Quantachrome Nova 2000 (Quantachrome Instruments, Boynton Beach, Florida, USA) surface area analyzer was used to measure the N_2 surface areas of the carboxylate-intercalated LDH samples that had been dried in air at 30ºC for 8 h to remove adsorbed water. After the thermogravimetric measurements, N_2 surface areas were measured again on LDH samples dried at 150ºC, which is the temperature of interlayer dehydration.

RESULTS AND DISCUSSION

Anion-exchange reactions

The nitrate anions in precursor LDH phases were easily exchanged with carboxylic acid anions. Most of the carboxylate anions were intercalated by anion exchange and no minor phases such as ZnO and sodium carboxylate were formed, but the heptadecanoic ($C_{17}H_{34}O_2$) and eicosanoic ($C_{20}H_{40}O_2$) acid anions could not be dissolved completely. Chemical composition and interlayer water were estimated by ICP and CHN elemental analyses and by TG, which confirmed that the M^{2+}/M^{3+} molar ratios were very close to the LDH-nitrate precursor values. This indicated that partial dissolution of the brucite-like main layers did not occur.

Examination by SEM showed morphology typical of organo-intercalated LDHs (Figure 1). The particles formed small platelets with rounded edges and diameters of up to 3 μm. The XRD powder patterns of wet samples had up to 11 sharp basal reflections that depended on the alkyl chain length of the carboxylate anions (Figure 2). No crystalline, nitrate-bearing LDH precursor phases were identified in any of the carboxylate-LDHs. The carboxylate-LDH c_0 values, which were three times greater than the d_{003} basal spacings, ranged from 3.4 to 13.5 nm, but the a_0 lattice parameter remained constant at 0.31 nm. The c_0 value increased linearly with carboxylate-anion alkyl-chain length, from the formate-LDH c_0 value of 3.4 nm with a $\Delta c'$ value of 0.11 nm/CH_3 without layer degradation. The $\Delta c'$ value doubled to 0.22 nm/CH_3 for carboxylate-LDHs with alkyl-chain lengths of >9 carbons. The carboxylate-ZnAl-LDH and precursor ZnAl-LDH cell parameters are compared in Figure 3 and Table 2. Drying at 35% r.h. decreased the structural order of the carboxylate-LDHs, primarily for 1- to 4-carbon alkyl-chain length carboxylate-LDHs (Figure 2, samples C1 and C3). The full width at half maximum (FWHM) of the basal reflection increased noticeably as intensity decreased. The basal peak was split into 2–3 separate reflections at greater 2θ angles. This disordering suggests that drying caused removal or re-orientation of the interlayer anions. Dried carboxylate-LDHs with carboxylate anions of >4 carbons had slightly smaller wet-sample basal spacings, indicating that structural order along the stacking direction was mostly retained. According to Itoh *et al*. (2003), organic anion chains are oriented in inclined monolayers or bilayers in LDH interlayers. The calculated average carboxylic acid alkyl chain angle was $\alpha_{CH_2\text{-chain}} = 60.7°$ for wet samples, which decreased slightly to 60.3° after drying at 35% r.h. Using the equation from Kopka *et al.* (1988)

$$c'_{cal} = 0.8 \text{ nm} + 0.127(n_C - 1)\sin\alpha_{CH_2\text{-chain}},$$

where n_C is the number of carbon atoms of the carboxylate anions, the theoretical basal spacings c'_{cal} were calculated (Figure 4), and these were 0.32–0.39 nm smaller than the experimentally determined spacings. Adding a monolayer of interlayer water molecules (0.31 nm) reduced these differences to 0.01–0.07 nm, in good agreement with the results from heating experiments by TG and XRD. The short alkyl-chain carboxylate anions formed monolayers in an inclined position in LDH interlayers. The slope of LDH basal spacings with longer alkyl-chain ($n_C > 9$) carboxylate anions increased to $\Delta c' = 0.22$ nm/CH_3, which is twice that for short alkyl-chain carboxylate-LDHs. The perpendicular interlayer anion orientation common for dicarboxylate anions can be excluded. Using the Meyn *et al*. (1990) model (Figure 4), the differences between calculated and experimental basal spacings are too large. The amount of interlayer water calculated from TG and chemical analyses do not support the existence of a second layer of interlayer water molecules (Table 1). The C and H contents of carboxylate-LDHs with carboxylates of $n_C > 9$ increased dramatically relative to the carboxylate-LDHs with carboxylates of $n_C < 9$. Based on a comparison between chemical analyses and basal spacings, the intercalated carboxylate anions probably have a bilayer orientation. Due to greater hydrophobic properties, larger aliphatic carboxylates can intercalate LDH interlayers in excess of the anion exchange capacity and form closely packed bilayer structures. The molecular packing depends on excess carboxylic acid and thermal treatment between 5 and 80ºC (Itoh *et al*., 2003). Carboxylate solution pH is another parameter that affects molecular packing. Anion-exchange experiments with selected carboxylic acids with $n_C > 10$ were performed at pH 4.0–5.0, 7.0, and 8.5. A carboxylic acid suspension equivalent to twice the anion exchange capacity of the LDH was heated to 45ºC under constant stirring and 1 M NaOH was added until the selected pH was reached. After mixing with the precursor LDH suspensions, samples were aged at 60ºC for 7 days. The basal peaks (d_{003} = 2.88 nm, d_{006} = 1.46 nm, d_{009} = 0.97 nm, d_{0012} =

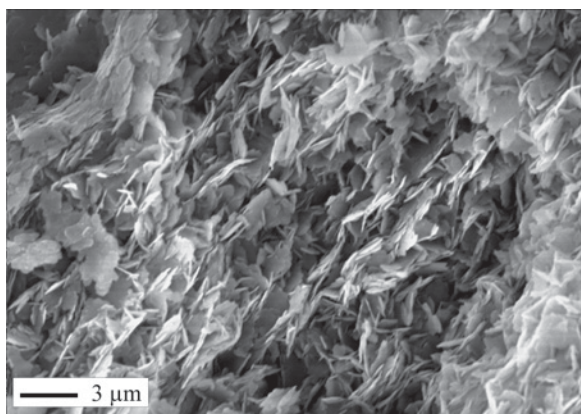

Figure 1. SEM image of ZnAl-pentanoate-LDH after drying at 35% r.h.

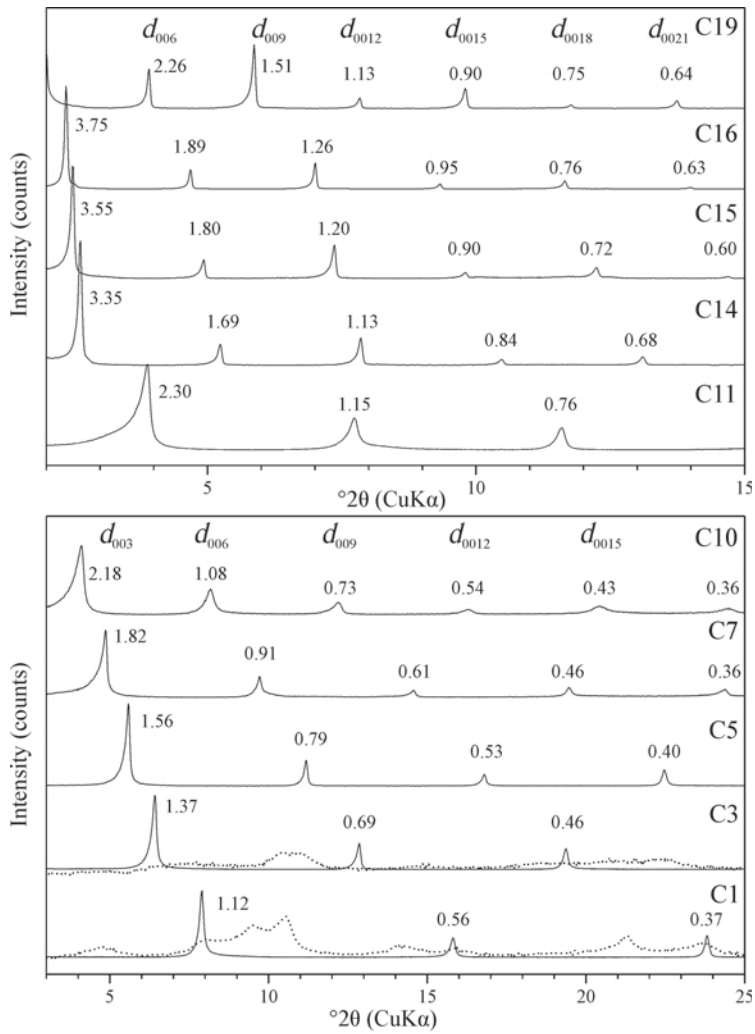

Figure 2. XRD patterns of selected carboxylate-LDHs at 100% r.h. (solid line, peak positions of d_{001} in nm) and at 35% r.h. (dotted line).

0.59 nm, d_{0015} = 0.49 nm, and d_{0018} = 0.42 nm) of ZnAl-dodecanoic hydrate shifted to larger 2θ angles as pH increased (Figure 5) and peak intensities decreased. The d_{003} plane reflection indicated that the interlayer distance increased from 2.4 nm at pH 8.5 to 2.9 nm at pH 4.5. Basal reflections of both series were observed at pH 7.0, which suggests that carboxylate anion monolayers form at high pH. The addition of NaOH to pH > 8.0 during preparation of the aqueous carboxylic acid suspension led to complete dissolution of the organic acid to yield a clear solution. The hydrophobic properties of carboxylic acids that cause bilayer formation were absent at higher pH. The carboxylic-acid sodium-salt reactant materials were initially at pH 8−9 and always led to a monolayer interlayer orientation. A monolayer LDH-interlayer orientation was favored under alkaline conditions, whereas the larger basal spacings under acidic conditions confirmed a bilayer arrangement. The formation of Na-carboxylate by the addition of excess aliphatic carboxylate (Itoh *et al.*, 2003) was not observed. All chemical analyses indicated Na contents of <0.5%.

The bilayer alkyl compound arrangement can be described by two different models (Lagaly, 1981). (1) The loss of one hydrogen ion per alkyl chain for each of the two interlayer organic molecules in the bilayer results in a negative interlayer charge twice that of the monolayer arrangement. (2) Only one of the two interlayer organic molecules forms an anion by the loss of a hydrogen ion and the other molecule is an undissociated acid. Chemical analyses and calculated LDH layer charges indicate that a second layer of undissociated acid in the interlayer results in a greater basal spacing. The FTIR spectra of selected LDH-carboxylates are composed of absorption bands from normal vibration modes that correspond to layer hydroxyl groups, carboxylate groups, hydroxyl groups, and Zn−O and Al−O stretching vibrations (Figure 6 and

Table 1. Results of chemical analyses (wt.%) for selected carboxylate-LDHs.

n_C	ZnO	Al_2O_3	C	H	H_2O
Carboxylic acid anion monolayer arrangement					
5	39.9	11.8	13.4	4.7	23.3
6	37.5	12.1	15.7	5.3	23.3
7	37.5	13.1	18.3	5.2	20.3
8	37.5	11.4	21.3	5.5	19.3
9	35.1	11.8	22.9	5.9	20.2
10	34.0	12.0	24.4	6.1	19.0
11	33.1	10.7	25.1	6.7	20.2
18	26.8	8.5	36.6	8.1	17.0
Carboxylic acid anion bilayer arrangement					
11	25.1	8.1	40.6	8.7	14.6
12	23.2	7.6	45.7	7.9	14.6
13	22.8	6.9	44.4	9.7	14.7
14	21.8	7.5	43.2	8.6	15.1
15	20.8	6.6	47.8	9.7	13.5
18	18.6	5.8	51.1	10.2	12.9
19	18.2	5.5	54.4	10.2	11.0

Table 3).The broad band centered at 3450 cm^{-1} is characteristic of all spectra and corresponds to the stretching vibrations of the hydration water. Intense bands are located at ~2930 cm^{-1} and 2850 cm^{-1}, assigned to symmetric and asymmetric stretching of CH_2 and CH_3. The weak band at 1600 cm^{-1} is generated by the ν_2(H-O-H) bending vibration of the interlayer water (Zhu *et al.*, 2008). The stretching bands ν(C=O) of the carboxylate functional groups give rise to absorptions at 1554 cm^{-1} and 1470 cm^{-1}, whereas the band at 1410 cm^{-1} overlaps the deformation vibrations δ(C-H) and δ(O-H). The band at 1554 cm^{-1} becomes generally more pronounced for hexanecarboxylate- to undecane-carboxylate LDHs and the interlayer water absorption band was less intense. Deformation vibrations from CH_2 and CH_3 are responsible for the weak bands in the 1200−1100 cm^{-1} region. Hydroxyl group translation modes influenced by main-layer Al formed significant

Table 2. Chemical formulae and lattice parameters (nm) of precursor ZnAl NO_3-LDH and carboxylate-LDH derivatives.

n_C[a]	Carboxylic acid anion salt		Idealized formula	a_0	c_0	c'
1	Formate		$[Zn_2Al(OH)_6][HCOO{\cdot}nH_2O]$	0.308	3.360	1.120
2	Acetate		$[Zn_2Al(OH)_6][CH_3COO{\cdot}nH_2O]$	0.308	3.816	1.272
3	Propanoate		$[Zn_2Al(OH)_6][C_2H_5COO{\cdot}nH_2O]$	0.308	4.125	1.375
4	Butanoate		$[Zn_2Al(OH)_6][C_3H_7COO{\cdot}nH_2O]$	0.308	4.506	1.502
5	Pentanoate		$[Zn_2Al(OH)_6][C_4H_9COO{\cdot}2.7H_2O]$	0.308	4.746	1.585
6	Hexanoate		$[Zn_2Al(OH)_6][C_5H_{11}COO{\cdot}3.0H_2O]$	0.308	5.193	1.731
7	Heptanoate		$[Zn_2Al(OH)_6][C_6H_{13}COO{\cdot}2.5H_2O]$	0.308	5.469	1.823
8	Octanoate		$[Zn_2Al(OH)_6][C_7H_{15}COO{\cdot}2.2H_2O]$	0.307	5.835	1.945
9	Nonanoate		$[Zn_2Al(OH)_6][C_8H_{17}COO{\cdot}2.8H_2O]$	0.307	6.171	2.057
10	Decanoate	(m.a.)	$[Zn_2Al(OH)_6][C_9H_{19}COO{\cdot}2.7H_2O]$	0.307	6.525	2.175
10	Decanoate	(b.a.)	$[Zn_2Al(OH)_6][(C_9H_{19}COO)\ (C_9H_{19}COOH){\cdot}nH_2O]$	0.307	7.503	2.501
11	Undecanoate	(m.a.)	$[Zn_2Al(OH)_6][C_{10}H_{21}COO{\cdot}3.2H_2O]$	0.307	6.881	2.293
11	Undecanoate	(b.a.)	$[Zn_2Al(OH)_6][(C_{10}H_{21}COO)(C_{10}H_{21}COOH){\cdot}2.8H_2O]$	0.308	8.162	2.721
12	Dodecanoate	(m.a.)	$[Zn_2Al(OH)_6][C_{11}H_{23}COO{\cdot}nH_2O]$	0.307	7.141	2.381
12	Dodecanoate	(b.a.)	$[Zn_2Al(OH)_6][(C_{11}H_{23}COO)(C_{11}H_{23}COOH){\cdot}3H_2O]$	0.307	8.779	2.926
13	Tridecanoate		$[Zn_2Al(OH)_6][(C_{12}H_{27}COO)(C_{12}H_{27}COOH){\cdot}3.2H_2O]$	0.307	9.420	3.140
14	Tertradecanoate		$[Zn_2Al(OH)_6][(C_{13}H_{27}COO)(C_{13}H_{27}COOH){\cdot}4H_2O]$	0.308	10.127	3.376
15	Pentadecanoate		$[Zn_2Al(OH)_6][(C_{14}H_{29}COO)(C_{14}H_{29}COOH){\cdot}3.2H_2O]$	0.307	10.848	3.616
18	Octadecanoate	(m.a.)	$[Zn_2Al(OH)_6][C_{17}H_{35}COO{\cdot}3.1H_2O]$	0.307	9.006	3.002
18	Octadecanoate	(b.a.)	$[Zn_2Al(OH)_6][(C_{17}H_{35}COO)(C_{17}H_{35}COOH){\cdot}3.5H_2O]$	0.307	12.698	4.233
19	Nonadecanoate		$[Zn_2Al(OH)_6][(C_{18}H_{37}COO)(C_{18}H_{37}COOH){\cdot}2.9H_2O]$	0.307	13.518	4.506
NO_3^-			$[Zn_2Al(OH)_6][NO_3{\cdot}1.9H_2O]$	0.308	2.678	0.893

[a] number of carbon atoms in the interlayer carboxylate anion
m.a. − monolayer arrangement, b.a.− bilayer arrangement of interlayer anions.

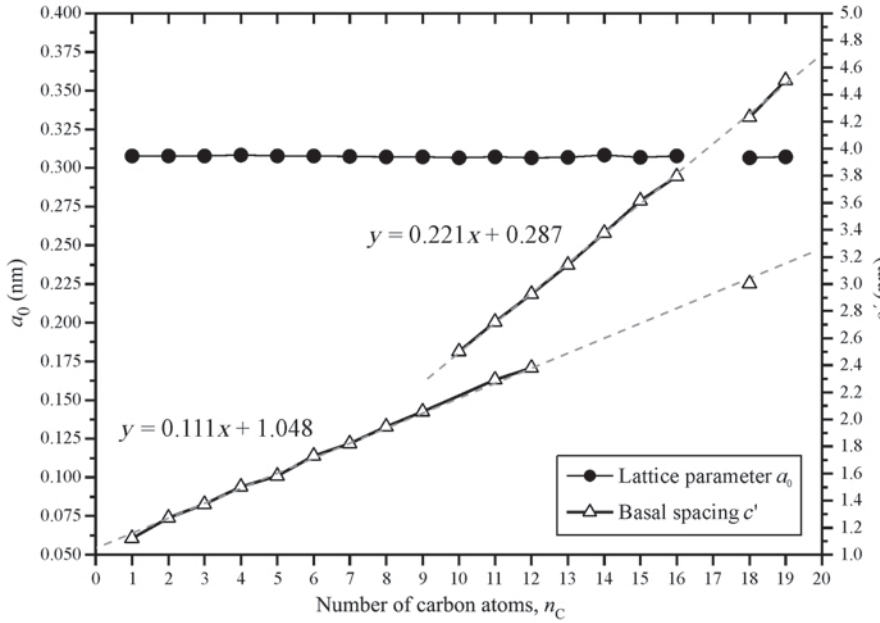

Figure 3. Interlayer space of ZnAl-LDHs depending on chain size of the incorporated carboxylate interlayer anions.

bands at ~770 cm^{-1}, 620 cm^{-1}, and 550 cm^{-1}. The small shoulder at 940 cm^{-1} is related to the Al–OH deformation vibration, whereas the Zn-OH translation mode is responsible for the intense band at 430 cm^{-1}. The significant carboxylate deformation and stretching bands and absence of a nitrate peak indicate complete exchange of nitrate by carboxylate anions. The FTIR spectra revealed no intercalated carbonate.

Thermogravimetric analyses of all samples were carried out under synthetic air and nitrogen flow to characterize different hydration stages and to further understand thermal decomposition reactions. The samples were dried to 35% r.h. before measurement. The TG curves obtained were very similar for all samples and showed a three-step degradation mechanism (Figure 7). The first step for ZnAl pentanoate-LDH, starting at 70ºC, resulted in a loss of 11.9% of the initial weight of the sample. Further heat treatment led to a second weight loss of 14.2% (230ºC), followed by a third weight loss, up to 520ºC. The ZnAl undecanoate-LDH thermogravimetric curve had a 7.8% weight loss step at 70–140ºC and further steps at 140ºC and at 207ºC. The thermograms are comparable to published LDH data (*e.g.* Anabarasan *et al.*, 2005; Reinholdt and Kirkpatrick,

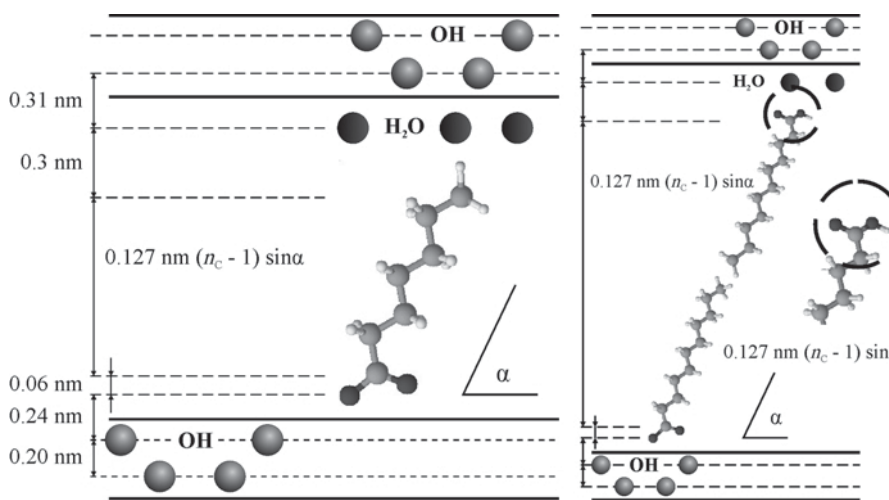

Figure 4. Models of the interlayer arrangement of aliphatic monocarboxylic acid anions: (a) monomolecular, (b) bimolecular (modified from Meyn *et al.*, 1990).

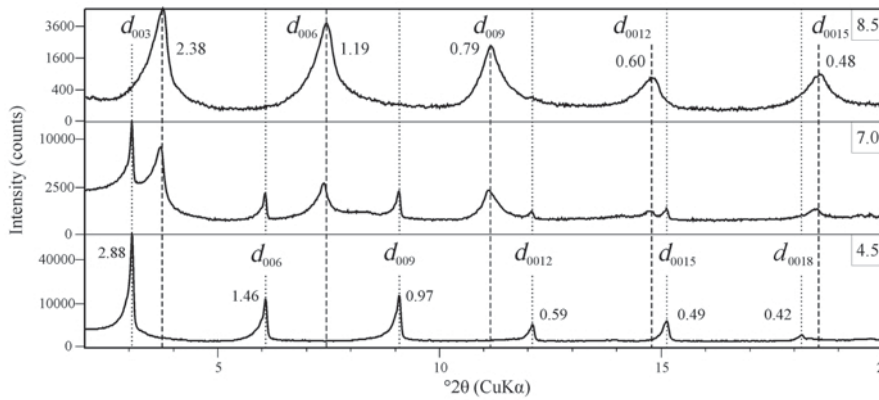

Figure 5. XRD patterns of ZnAl-dodecanoate-LDH at different initial pH values of the carboxylic acid solutions (peak positions of d_{001} in nm).

2006). The first mass loss is due to the low-temperature removal of surface water (28−70ºC) and interlayer water molecules. The calculated interlayer water was equivalent to 0.9 mol H_2O per formula unit for ZnAl pentanoate-LDH and 0.87 mol H_2O for ZnAl undecanoate-LDH. The calculated water contents are in good agreement with chemical data from CHN element analysis. Dehydroxylation of the brucite-like main layers, with subsequent collapse of the layered structure, is attributed to the second step. The last process can be divided into two separate steps. At temperatures above 210ºC, dehydroxylation and interlayer anion decomposition takes place, followed by ZnO, and later, $ZnAlO_4$ spinel formation.

The BET specific surface areas ranged from 1.2 to 13 $m^2\ g^{-1}$ for the hydrated carboxylate-LDH samples (S_{BET}, Table 4). The hydrated surface areas of the different carboxylate-LDHs differ, but no clear relationship was evident between carboxylate alkyl chain length and surface area. The smallest BET surface area was measured for ZnAl nonanoate-LDH (1.2 $m^2\ g^{-1}$); the largest, for the ZnAl stearate-LDH (13 $m^2\ g^{-1}$), was in good agreement with the BET surface area of MgAl stearate-LDH, of 12.9 $m^2\ g^{-1}$ (Nhlapo *et al*., 2008). Thermal treatment to 140−150ºC removed interlayer water and increased specific surface area, especially for the LDHs with short alkyl-chain mono-carboxylic acid anions. The small S_{BET} values were possibly related to the large crystal size (<3 μm) and to the common aggregation of the single crystals (Figure 1).

Thermal treatment of the ZnAl-organic derivates

Based on thermogravimetric analyses, XRD was used to examine the ZnAl-LDH-carboxylates over the tem-

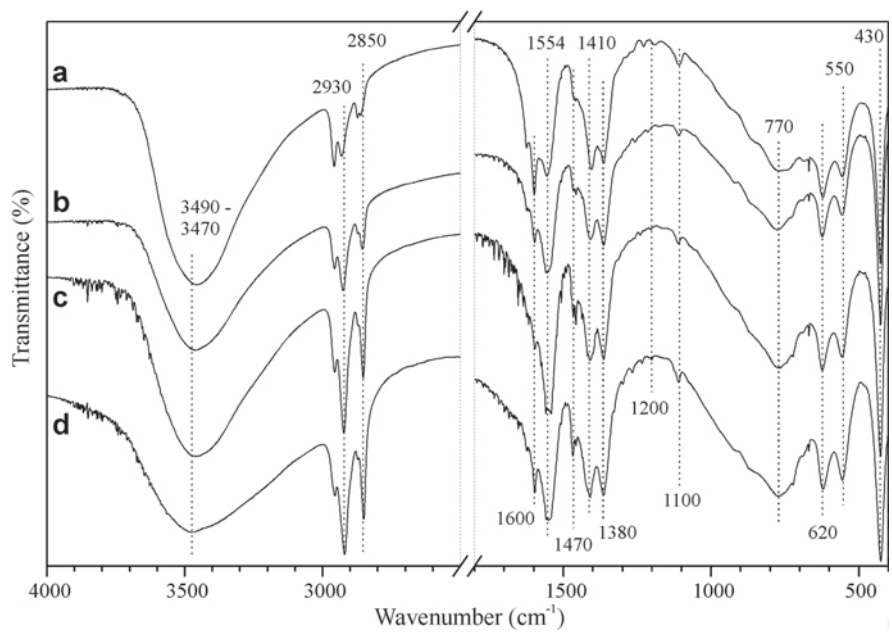

Figure 6. FTIR spectra of (a) ZnAl-$C_6H_{11}O_2^-$, (b) ZnAl-$C_8H_{15}O_2^-$, (c) ZnAl-$C_{10}H_{19}O_2^-$, (d) ZnAl-$C_{11}H_{21}O_2^-$.

Table 3. Peak assignments for carboxylate-LDH infrared bands.

Band (cm^{-1})	Type of vibration	
3490−3470	$N_{1,3}(H_2O)$	(H−O−H) stretching vibration of hydroxyl groups
2930−2850	$\nu_s(CH_2, CH_3)$	Symmetrical and asymmetrical stretching of CH_2 and CH_3 groups
1600	$\nu_2(H_2O)$	Sorbed water
1554, 1470	ν(C=O)	Stretching vibration of carboxylate functional groups
1410	δ(C−H), δ(O−H)	Deformation band (C−H)
1380−1360	$\delta_s(CH_3)$	Symmetrical deformation vibration of CH_3 groups
1200−1100	$\delta(CH_2)$	Deformation vibrations CH_2 and CH_3 groups
770, 620, 550	δ(*Me*−OH)	(*Me*−OH) deformation band and (Al^{IV}−O) vibration
430	ZnO	Zn−O vibration

perature range 25−300ºC in a heating chamber. Prior to XRD examination, the LDH samples were prepared as wet pastes (35% r.h.) with a few drops of acetone added to form an homogeneous layer on the sample holder. Based on the XRD powder patterns, the carboxylate-LDHs were divided into two groups with either a monolayer or bilayer orientation of the intercalated carboxylate. A plot that combined a thermogravimetric weight loss curve with the XRD basal spacings for ZnAl-LDH-$C_5H_9O_2$ was characteristic of other LDH-carboxylates with $n_C < 10$ alkyl chains and a monolayer interlayer arrangement (Figure 8). Heating from 25 to 70ºC decreased the basal spacing (c') slightly, from 1.58 to 1.54 nm, due to the removal of superficially adsorbed water. The first major TG-curve weight-loss step at 70ºC was accompanied by a strong basal spacing decrease to 1.31 nm, which indicates interlayer water removal and minor simultaneous reorientation of the interlayer carboxylate anions to a more inclined position in the interlayer. The XRD powder patterns of dehydrated, short alkyl-chain carboxylate-

Table 4. Specific surface areas of selected carboxylate-LDHs and precursor nitrate-LDH.

ZnAl-	n_C	S_{BET} ($m^2\ g^{-1}$) at different outgassing temperatures	
		30ºC	150ºC
Formate	1	6.1	19.7
Acetate	2	9.0	28.5
Propionate	3	2.5	31.6
Pentanoate	5	12.8	29.7
Hexanoate	6	5.6	22.2
Heptanoate	7	5.1	18.5
Octanoate	8	10.4	12.9
Nonanoate	9	1.2	2.4
Decanoate	10	4.7	7.0
Tetradecanoate	14	9.8	3.2
Stearate	18	13.0	7.2
Nitrate precursor		5.2	6.6

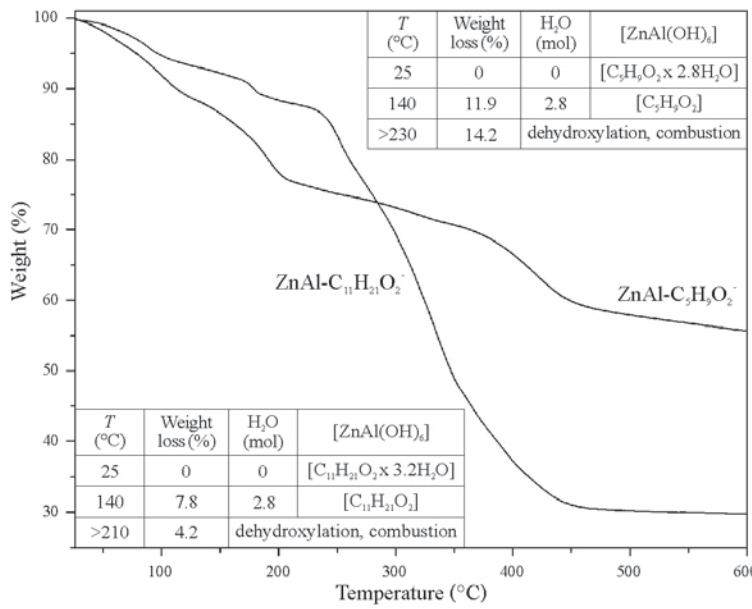

Figure 7. TG curves of ZnAl pentanoate-LDH and ZnAl undecanoate-LDH^- with a temperature step where interlayer water was removed.

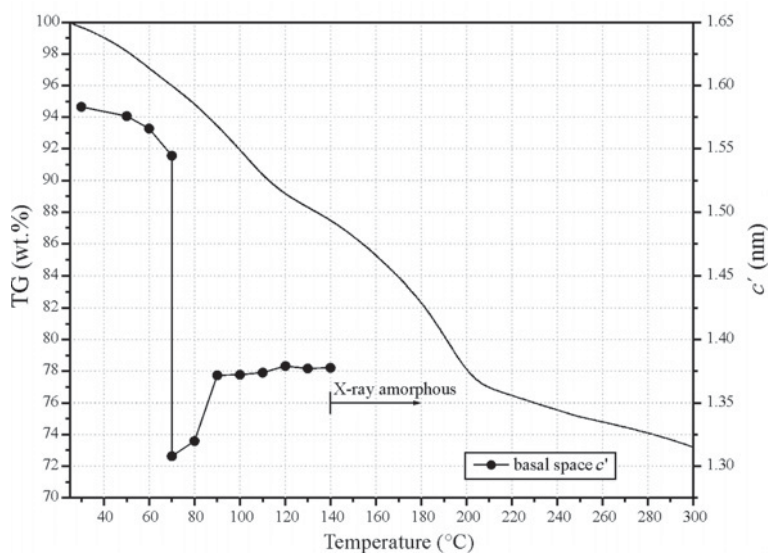

Figure 8. TG curve *vs*. basal spacing of ZnAl pentanoate-LDH.

LDHs (not shown) had broad, low-intensity basal reflections, which indicated major disorder of the interlayer carboxylate anions. An increased temperature led to a more upright orientation of the carboxylate anions until crystal structure collapse at 140ºC when the carboxylate-LDH became X-ray amorphous.

The carboxylate-LDHs, with $n_C > 10$ alkyl-chain lengths behaved differently. (1) The TG curve revealed a constant weight loss from 25−130ºC with minor weight-loss steps characteristic of short alkyl-chain carboxylate-LDHs. (2) The basal spacing of ZnAl-LDH-$C_{19}H_{37}O_2$ expanded from 4.48 nm (25ºC) to 4.60 nm (125ºC), which was evident from a continuous shift of the d_{003} basal spacing to smaller 2θ angles as the temperature was increased. Furthermore, the basal reflection intensities increased from 25 to 50ºC (Figure 9). This behavior was observed for all long alkyl-chain carboxylate-LDHs with a bilayer orientation. Based on the XRD patterns of short-alkyl chain carboxylate-LDHs, the d_{003} shifts can be interpreted as re-orientation of interlayer carboxylate molecules from an inclined to a more upright position until the main layers dehydroxylated. Alternatively, the large basal spacing is related to stretching of the alkyl chain during heat treatment. However, further studies are needed to analyze this behavior. The CHNS analyses of heated samples gave no evidence of late interlayer carbonation, but neither did they reveal removal of any interlayer water. The large peak intensities and moderate peak widths indicate a well ordered interlayer arrangement within the temperature range examined.

CONCLUSIONS

The anion exchange of saturated, aliphatic carboxylate anions with ZnAl-LDHs were analyzed as a function of synthesis temperature, time, pH, and carboxylate alkyl-chain length. The precursor ZnAl-

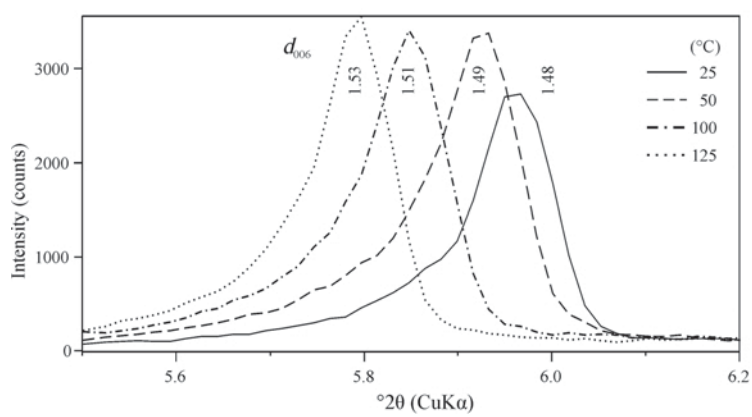

Figure 9. Position of d_{006} basis reflection (nm) of ZnAl nonadecanoate-LDH at different temperatures.

NO_3 LDH phases were well suited to anion-exchange reactions with carboxylate anions. All carboxylate anions were added in excess of the LDH anion exchange capacity to ensure complete anion exchange. The excess amount of carboxylate anion decreased as carboxylate alkyl-chain length increased. The basal spacing increased as the carboxylate anion size increased, as reported for other organic molecules. The $n_C < 10$ carboxylate anions were generally arranged into monolayers. Depending on the pH during anion exchange, long alkyl-chain carboxylates formed monolayers or bilayers in LDH interlayers. In addition to synthesis temperature and carboxylate anion excess, the hydrophobic properties of the undissociated carboxylic acid appear to be explained by a bilayer orientation. Thermal treatment of the LDHs yielded useful information about stability, interlayer water behavior, and interlayer size, which are important for LDH use as a catalyst. The short alkyl-chain carboxylate-LDHs had typical interlayer water-removal weight-loss steps with simultaneous decreases in basal spacing. The greater basal spacings of the long alkyl-chain carboxylate-LDHs is complex and needs more detailed study.

ACKNOWLEDGMENTS

The authors thank Prof. Richard Wenda, Dr Stefan Stoeber, and Dr Robert Mikutta for support and helpful discussions concerning the XRD experiments and the BET isotherm measurements. The anonymous reviewers are acknowledged for helping to improve the quality of this paper.

REFERENCES

Anbarasan, R., Lee, W.D., and Im, S.S. (2005) Adsorption and intercalation of anionic surfactants onto layered double hydroxides – XRD study. *Bulletin of Materials Science*, **28**, 145–149.

Bish, D.L. (1980) Anion-exchange in takovite: applications to the other hydroxide minerals. *Bulletin of Mineralogy*, **103**, 170–175.

Carlino, S. (1997) The intercalation of carboxylic acids into layered double hydroxides: a critical evaluation and review of the different methods. *Solid State Ionics*, **98**, 73–84.

Cavani, F., Trifiro, F., and Vaccari, A. (1991) Hydrotalcite-type anionic clays: Preparation, properties and applications. *Catalysis Today*, **11**, 173–301.

Choudhary, V.R., Dumbre, D.K., Narkhede, V.S., and Jana, S.K. (2003) Solvent-free selective oxidation of benzyl alcohol and benzaldehyde by tert-butyl hydroperoxide using MnO_4-exchanged Mg-Al-hydrotalcite catalysts. *Catalysis Letters*, **86**, 229–233.

Cooper, M.A. and Hawthorne, F.C. (1996) The crystal structure of shigaite, $[AlMn_2^{2+}(OH)_6]_3(SO_4)_2$ $Na(H_2O)_6\{H_2O\}_6$, a hydrotalcite-group mineral. *The Canadian Mineralogist*, **34**, 91–97.

Hansen, B., Curtius, H., and Odoj, R. (2009) Synthesis of a Mg-Cd-Al layered double hydroxide and sorption of selenium. *Clays and Clay Minerals*, **57**, 330–337.

Itoh, T., Ohta, N., Shichi, T., Yui, T., and Takagi, K. (2003) The self-assembling properties of stearate ions in hydrotalcite clay composites. *Langmuir*, **19**, 9120–9126.

Khan, A.I. and O'Hare, D. (2002) Intercalation chemistry of layered double hydroxides: recent developments and applications. *Journal of Materials Chemistry*, **12**, 3191–3198.

Kloprogge, J.T., Wharton, D., Hickey, L., and Frost, R.L. (2002) Infrared and Raman study of interlayer anions CO_3^{2-}, NO_3^-, SO_4^{2-} and ClO_4^- in Mg/Al-hydrotalcite. *American Mineralogist*, **87**, 623–629.

Kopka, H., Beneke, K., and Lagaly, G. (1988) Anionic surfactants between double metal hydroxide layers. *Journal of Colloid and Interface Science*, **123**, 427–436.

Lagaly, G. (1981) Inorganic layer compounds. *Naturwissenschaften*, **68**, 82–88.

Meyn, M., Beneke, K., and Lagaly, G. (1990) Anion-exchange reactions of layered double hydroxides. *Inorganic Chemistry*, **29**, 5201–5207.

Nhlapo, N., Motumi, T., Landman, E., Verryn, A.M.C., and Focke, W.W. (2008) Surfactant-assisted fatty intercalation of layered double hydroxides. *Journal of Materials Science*, **43**, 1033–1043.

Ogawa, M. and Kaiho, H. (2002) Homogeneous precipitation of uniform hydrotalcite particles. *Langmuir*, **18**, 4240–4242.

Poellmann, H. (2007) *Immobilisierung von Schadstoffen durch Speichermineralbildung*. Shaker-Verlag, Achen, Germany, pp. 130–150.

Prasanna, S.V., Radha, A.V., Kamath, P.V., and Kannan, S. (2009) Bromide-ion distribution in the interlayer of the layered double hydroxides of Zn and Al: Observation of positional Disorder. *Clays and Clay Minerals*, **57**, 82–92.

Reichle, W.T. (1986) Synthesis of anionic clay minerals (mixed metal hydroxides, hydrotalcite). *Solid State Ionics*, **22**, 135–141.

Reinholdt, M.X. and Kirkpatrick, R.J. (2006) Experimental investigations of amino acid-layered double hydroxide complexes: glutamate-hydrotalcite. *Chemistry of Materials*, **18**, 2567–2576.

Roy, A., Forano, C. and Besse, J.P. (2001) Layered double hydroxides: Synthesis and postsynthesis modifications. Pp. 1–38 in: *Layered Double Hydroxides: Present and Future* (V. Rives, editor). Nova Science Publishers, Inc., New York.

Wypych, F., Arízaga, G.G.C., and da Costa Gardolinski, J.E.F. (2005) Intercalation and functionalization of zinc hydroxide nitrate with mono- and dicarboxylic acids. *Journal of Colloid and Interface Science*, **283**, 130–138.

Xu, Z.P. and Bratermann, P.S. (2007) Competitive Intercalation of Sulfonates into Layered Double Hydroxides (LDHs): the Key Role of Hydrophobic Interactions. *Journal of Physical Chemistry C*, **111**, 4021–4026.

Yang, L., Sharivari, Z., Liu, P.K.T., Sahimi, M., and Tsotsis, T.T. (2005) Removal of trace levels of arsenic and selenium from aqueous solutions by calcined and uncalcined layered double hydroxides (LDH). *Industrial & Engineering Chemical Research*, **44**, 6804–6815.

Zhao, H. and Vance, G.F. (1998) Selectivity and molecular sieving effects of organic compounds by a β-cyclodextrin-pillared layered double hydroxide. *Clays and Clay Minerals*, **46**, 712–718.

Zhu, J., Yuan, P., He, H., Frost, R., Tao, Q., Shen, W., and Bostrom, T. (2008) In situ synthesis of surfactant/silane-modified hydrotalcites. *Journal of Colloid and Interface Science*, **319**, 498–504.

(*Received 1 July 2009; revised 4 August 2010; Ms. 331; A.E. W.F. Jaynes*)